0161-4754/99/$8.00 + 0 **76/1/95617** © 1999 JMPT

Validation of the Force and Frequency Characteristics of the Activator Adjusting Instrument: Effectiveness as a Mechanical Impedance Measurement Tool

Tony S. Keller, PhD,[a] Christopher J. Colloca, DC,[b] and Arlan W. Fuhr, DC[c]

ABSTRACT

Objective: To determine the dynamic force-time and force-frequency characteristics of the Activator Adjusting Instrument and to validate its effectiveness as a mechanical impedance measurement device; in addition, to refine or optimize the force-frequency characteristics of the Activator Adjusting Instrument to provide enhanced dynamic structural measurement reliability and accuracy.

Methods: An idealized test structure consisting of a rectangular steel beam with a static stiffness similar to that of the human thoracolumbar spine was used for validation of a method to determine the dynamic mechanical response of the spine. The Activator Adjusting Instrument equipped with a load cell and accelerometer was used to measure forces and accelerations during mechanical excitation of the steel beam. Driving point and transfer mechanical impedance and resonant frequency of the beam were determined by use of a frequency spectrum analysis for different force settings, stylus masses, and stylus tips. Results were compared with beam theory and transfer impedance measurements obtained by use of a commercial electronic PCB impact hammer.

Results: The Activator Adjusting Instrument imparted a very complex dynamic impact comprising an initial high force (116 to 140 N), short duration pulse (<0.1 ms) followed by several lower force (30 to 100 N), longer duration impulses (1 to 5 ms). The force profile was highly reproducible in terms of the peak impulse forces delivered to the beam structure (<8% variance). Spectrum analysis of the Activator Adjusting Instrument impulse indicated that the Activator Adjusting Instrument has a variable force spectrum and delivers its peak energy at a frequency of 20 Hz. Added masses and different durometer stylus tips had very little influence on the Activator Adjusting Instrument force spectrum. The resonant frequency of the beam was accurately predicted by both the Activator Adjusting Instrument and electronic PCB impact hammer, but variations in the magnitude of the driving point impedance at the resonant frequency were high (67%) compared with the transfer impedance measurements obtained with the electronic PCB impact hammer, which had a more uniform force spectrum and was more repeatable (<10% variation). The addition of a preload-control frame to the Activator Adjusting Instrument improved the characteristics of the force frequency spectrum and repeatability of the driving point impedance measurements.

Conclusion: These findings indicate that the Activator Adjusting Instrument combined with an integral load cell and accelerometer was able to obtain an accurate description of a steel beam with readily identifiable geometric and dynamic mechanical properties. These findings support the rationale for using the device to assess the dynamic mechanical behavior of the vertebral biomechanical effectiveness of various manipulative, surgical, and rehabilitative spinal procedures. (J Manipulative Physiol Ther 1999;22:75-86)

Key Indexing Terms: Spine; Biomechanics; Chiropractic Manipulation

INTRODUCTION

Knowledge of spine segment, or functional spinal unit (FSU), motion patterns (kinematics) and forces (kinetics) is of importance for understanding the response of the spine to externally applied forces such as spinal manipulative therapy (SMT). SMT is generally considered to be therapeutic, but little is understood regarding the mechanisms of its positive treatment effects. To understand the biomechanical consequences of SMT more fully researchers are currently focusing on quantifying the applied forces and the response of the spine to these forces.[1-11]

During SMT, posterior to anterior (PA) forces can range from 50 to 550 N, depending on the procedure used.[1-11] Preload forces during these procedures can be as low as 20 N or as high as 200 N. In general, higher peak forces (up to 550 N) are associated with SMT of the sacroiliac joint, whereas lower peak forces have been demonstrated in SMT of the cervical spine.

In principle, a dysfunctional or unstable FSU may exhibit increased displacement or decreased stiffness compared with adjacent segments.[12] Consequently, the displacement of the FSU and the resistance of spinal tissues to applied forces during SMT may be potentially very useful in spinal diagnosis and for establishing effective treatment protocols. Ideally, measurements of the mechanical response of the

[a]Professor, Department of Mechanical Engineering, University of Vermont, Musculoskeletal Research Laboratory, Burlington, Vermont.

[b]Postdoctoral and Related Professional Education Department Faculty, Logan College of Chiropractic, St. Louis, Missouri; private practice of chiropractic, Phoenix, Arizona.

[c]President, Activator Methods, Inc; private practice of chiropractic.

Submit reprint requests to: Dr Christopher J. Colloca, State of the Art Chiropractic Center, PC, 11011 S 48th St, Suite 205, Phoenix, AZ 85044.

Paper submitted March 16, 1998.

Supported by the National Institute of Chiropractic Research and Logan College of Chiropractic.

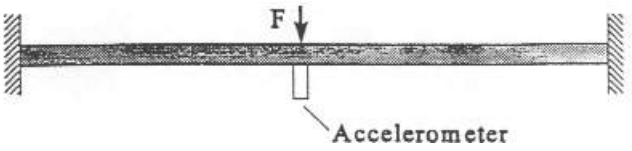

Fig 1. *Schema of structural beam used to mimic static PA stiffness and dynamic frequency characteristics of human lumbar spine.* F, *Force.*

Table 1. *Summary of frequency response functions*

Accelerance	Output acceleration/input force
Effective mass	Input force/output acceleration
Mobility	Output velocity/input force
Impedance	Input force/output velocity
Dynamic compliance	Output displacement/input force
Dynamic stiffness	Input force/output displacement

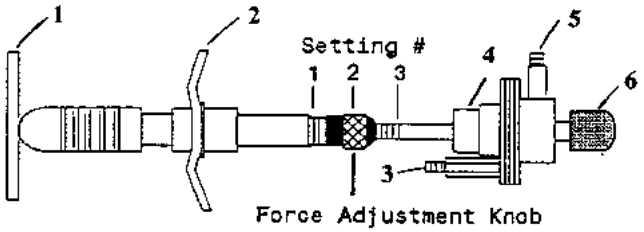

Fig 2. *AAI with labeled parts, including integral force and acceleration sensors. Adjustable force adjustment knob allows different excursions of instrument. Setting No. 1 (1 ring showing on instrument); setting No. 2 (midway or center point of excursion); setting No. 3 (adjustment knob opened as far as possible for maximum excursion). Parts of AAI are labeled: second handle member* (1), *first handle member* (2), *accelerometer* (3), *impact stylus* (4), *load cell* (5), *rubber tip* (6).

FSU should be accomplished by use of a procedure wherein motions and forces are measured in vivo and directly on the spinal structures, but such measurements generally necessitate an invasive procedure. Consequently, numerous in vitro measurements of spinal kinematics and kinetics have been performed, but few measurements of in vivo static and dynamic stiffness characteristics of the spine have been reported in the literature.

Relative sagittal plane motions of human lumbar FSUs have been quantified in vivo during SMT by use of an intervertebral motion device in 3 subjects.[7] The intervertebral motion device consisted of Steinmann pins attached directly into the L3-L4 and L4-L5 spinous processes connected by a strain gauge apparatus system.[7] These investigators were the first to quantify the in vivo motion characteristics of the human lumbar FSU during SMT and noted that high-velocity (up to 1 ms^{-1}) PA adjustments applied to the L2 spinous process with an Activator Adjusting Instrument (AAI) (Activator Methods, Inc, Phoenix, Ariz) produced relative PA displacements, axial displacements, and sagittal rotations of adjacent FSUs ranging from 0.1 to 0.5 mm, 0.3 to 1.6 mm, and 0.2 to 0.9 degrees during the application of peak forces ranging from 48 to 123 N. In this case, we are using the term "relative" to refer to the fact that the intervertebral motion device is a spatial linkage or goniometer type of device that measures relative displacements and rotations between vertebrae and not the absolute displacement of a single vertebrae. Gál and associates[9] recently reported the relative movements of thoracic vertebrae during PA adjustments of 2 unembalmed cadavers. Using a low-speed cinematography technique, they reported similar relative PA translations, lateral translations, axial rotations, and sagittal rotations ranging from 0.00 to 0.45 mm, 0.01 to 0.42 mm, 0.00 to 0.20 degrees, and 0.15 to 028 degrees, respectively, during application of 509 to 562 N peak forces to the right transverse processes of T10-T12. Although these studies provide convincing evidence that SMT procedures produce substantial movements of the FSU, the fact that substantially different force amplitudes produce similar movements in human vertebrae suggests that the dynamic mechanical characteristics of SMT procedures may play an important role in the ensuing FSU motion and concomitant physiologic response(s). Others have noted similar disparities when comparing, for example, PA translations of human cadaver and animal lumbar FSUs to so-called high-force and low-force SMT, respectively, but have attributed such findings to differences in the direction of the applied force and/or intrinsic anatomic and species-specific differences.[9]

In the in vivo study by Nathan and Keller,[7] the recorded vertebral motions were higher in the normal subject examined compared with subjects with an L4-L5 retrospondylolisthesis or L4-L5 degenerated disk. Of interest was the finding that vertebral stiffness derived from noninvasive mechanical impedance (force-velocity) measurements at the site of applications of the SMT impulse showed a close correspondence to the sagittal plane intervertebral motion device motion measurements of adjacent segments. Segments with higher intervertebral displacement and rotation exhibited decreased mechanical impedance (increased stiffness). This indicated that PA force-acceleration measurements may be a valid method to probe the mechanical behavior of the human spine and other structures noninvasively, which has motivated this study.

The primary objectives of this study were to characterize the dynamic force-time and force-frequency characteristics of the AAI and to validate the effectiveness of the use of an AAI to quantify the dynamic mechanical behavior of a well-defined engineering structure. A second goal was to refine or optimize the force-frequency characteristics of the AAI to provide enhanced dynamic structural measurement reliability and accuracy.

MATERIALS AND METHODS

Experimental Setup

For this experiment, a steel beam was selected that would approximate the static PA stiffness (10 to 200 kN/m) and first natural frequency (50 Hz) of the normal human lumbar FSU.[7,13] The beam had a uniform square cross-section of 11.43 mm per side and was rigidly fixed at both ends, 1 m apart. The rigid constraints applied to the beam approxi-

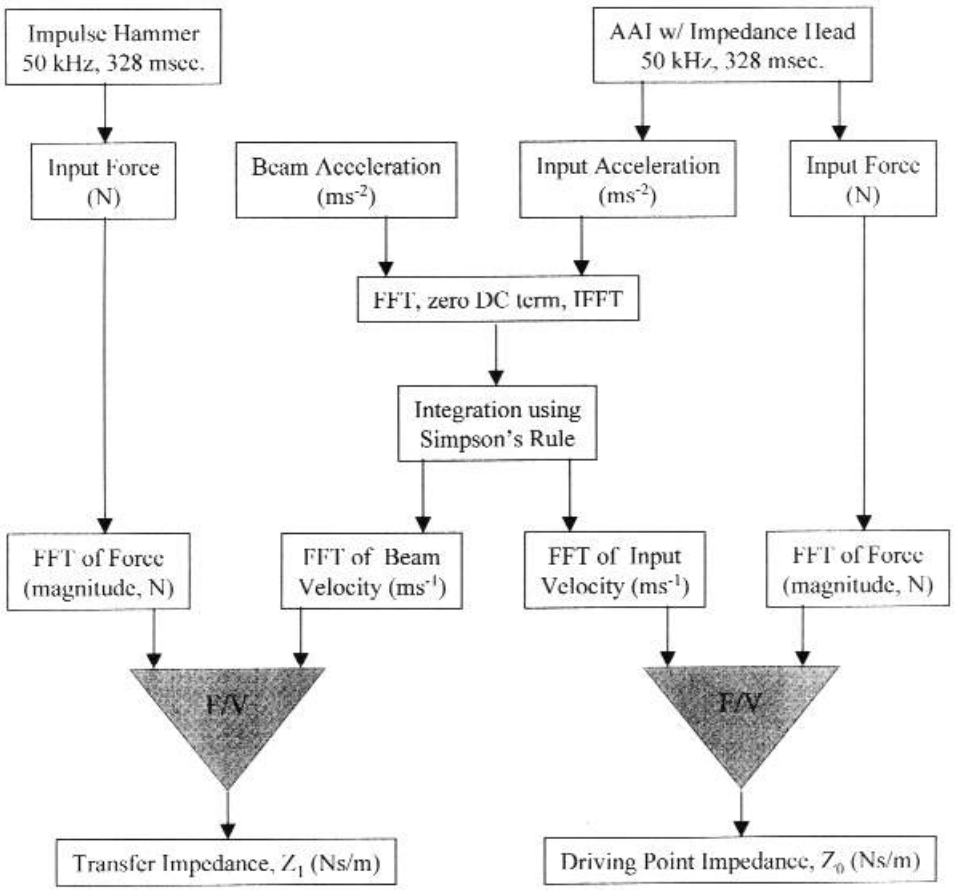

Fig 3. *Summary of data acquisition and impedance data analysis procedure.*

mate the manner in which the normal human spine is constrained at the pelvis and rib cage. By rigidly fixing the beam, a force applied perpendicular to the long axis of the beam will induce an axial force within the beam, not unlike that which occurs during the application of PA thrusts to the spine.

Young's modulus and structural stiffness of the steel beam were determined experimentally by applying a series of loads (P, kg) to the center of the beam and recording the resulting deflections (δ, m). The structural stiffness (kN/m) was defined as the slope of the load versus deflection curve (P/δ). Young's modulus (E, Pa) was computed by use of the following beam deflection equation:

$$E = -\frac{P}{\delta}\,\frac{L^3}{192I}$$

where L is the length of the beam between the end supports and I is the area moment of inertia (1422 mm^4). Loads ranging from 10 to 100 N were applied, and the resulting deflections were measured by means of a dial gauge with an accuracy of 2.5 μm. Young's modulus and the structural stiffness obtained from the static deflection tests were 167 GPa and 45.6 kN/m, respectively.

The natural frequency f_n of this beam configuration is given by:

$$fn = \frac{Kn}{2\pi}\sqrt{\frac{EI}{WL^4}}$$

where K_n = 22.4 for mode 1 vibrations, W is the mass per unit length of the beam (0.96 kg/m), and the other parameters are defined previously. Using this simple equation together with the modulus calculated from the static deflection tests, the theoretical first natural frequency was determined to be 56.1 Hz for a beam 1 m long. Note that the preceding equations assume that the beam is an elastic and isotropic material.

An accelerometer (model 305A04, PCB Piezotronics, Inc, Depew, NY) was attached to the beam at the center point between the 2 supports (Fig 1). The accelerometer has a sensitivity of 1 mV/g, 5000g range and resonant frequency of 60 kHz. Two different devices were used to deliver forces to the beam: an AAI and an electric PCB impact hammer (PCB) (model 086C09, PCB Piezotronics, Inc, Depew, NY). The AAI delivers a very short duration (<5 ms) force-time impulse with a peak force magnitude of about 150 N.[14] The AAI remains in contact with the structure during use and can be preloaded. The PCB has an integral driving point force sensor with an adjustable force sensor, with an adjustable force range of about 200 to 5000 N and produces a near perfect half sine wave impulse (approximately 150 ms duration) without preloading the beam. Fig 2 shows the

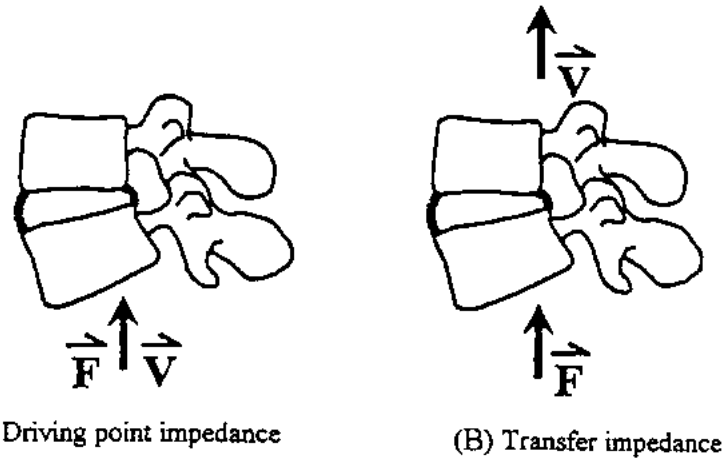

Fig 4. *Schema of force-velocity relationship for driving point impedance (Z_0)* ***(A)*** *and transfer impedance (Z_1)* ***(B)***.

configuration of the AAI with attached force and acceleration sensors.

Data Acquisition

Data from the load cells (attached to the PCB and the AAI) and the accelerometers (attached to the beam and the AAI) were collected with a 12-bit A/D converter connected to a Macintosh II computer. A total of 16,384 samples of data per channel was acquired at a sampling frequency of 50 kHz (20 μs/sample), resulting in a total sample duration of about 328 ms. Data were obtained for 10 trials at a fixed beam length of 1 m. For each trial the impact was delivered to the center point between the end supports. A 30-durometer tip (30d) was attached to the AAI, and a slight preload (<10 N) was used for these trials. Durometer was specified by means of the ASTM D-2240 designation and refers to the "hardness" of the various rubber tips attached to the stylus of the AAI. The preload was applied manually in a manner consistent with routine clinical use of the AAI instrument. The impedance head attached to the AAI contributed an additional 34 g to the mass of the standard AAI stylus and hammer (46 g).

AAI impacts were also applied to the beam with different durometer tips, added masses, and force settings as follows:

1. Two different AAI force settings: 1 (minimum) and 3 (maximum) in Fig 1.
2. Four different durometer tips were examined: 30d, 50d, 70d, and 80d.
3. Three different masses (using an 80-d tip): 0 g (m0), 249 g (m1), and 386 g (m2).

Five trials were obtained for each of the preceding 3 cases. AAI input load and input acceleration were acquired at a sampling frequency of 50 kHz.

Data Analysis

Peak input load, input and beam acceleration, and input and beam velocity were computed for each of the 10 PCB impacts and t30d AAI impact trials, and standard descriptive statistics were performed.

The load-time and acceleration-time data were further analyzed in the frequency domain with LabViews software (National Instruments Corp, Austin, Tex). Fig 3 illustrates the steps involved in the analysis, which begins by converting the time-domain signals into frequency-domain signals with a fast Fourier transform (FFT). For this study, the main parameters of interest were the magnitude of dynamic mechanical impedance (Z) and first natural frequency (resonance) of the structure. Mechanical impedance is defined as the ratio of force magnitude/velocity magnitude and thus required computation of the velocity that was obtained by integrating the acceleration signal. Magnitude refers to the square root of the sum of the squares of the real and imaginary terms produced by the FFT analysis. Resonance or increased oscillation occurs when the impedance magnitude approaches zero and is generally characterized as a valley in the impedance magnitude versus frequency plot. Because accelerometers were attached to both the beam and AAI impedance head, 2 types of mechanical impedance could be calculated: driving point impedance and transfer impedance. Driving point impedance (Z_0) is defined as the ratio of the magnitude of the input force/input velocity in the frequency domain:

$$Z_0 = \text{FFT (input force)}/\text{FFT (input velocity)}$$

where input velocity is the velocity derived from the AAI accelerometer. Transfer impedance (Z_1) is defined as the ratio of the magnitude of input force/response velocity in the frequency domain:

$$Z_1 = \text{FFT (input force)}/\text{FFT (response velocity)}$$

where response velocity is the velocity derived from the accelerometer attached directly to the beam. Both driving point and transfer impedance were calculated for the AAI impacts, whereas only transfer impedance was determined for the PCB impacts. Fig 4 illustrates the difference between driving point and transfer impedance. Table 1 provides a complete inventory of frequency response functions.

For the 10 PCB impacts and 10 AAI impacts, the transfer impedance was calculated and plotted as a function of fre-

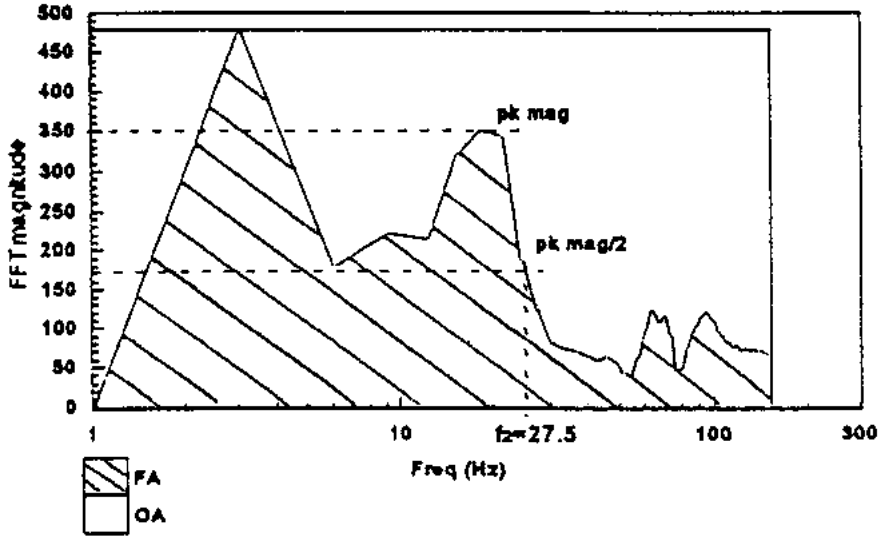

Fig 5. *Illustration of method used to determine input force characteristics of AAI and PCB impulse hammer. Two parameters were measured from each force magnitude versus frequency plot: (1) frequency f_{50} at which the greater than 10 Hz peak magnitude was reduced by 3 dB (50%) and (2) relative input force magnitude or ratio of force applied/overall force (FA/OA) over frequency range 3 to 150 Hz.*

Table 2. *Peak forces, accelerations, and velocities obtained from PCB impulse hammer and AAI impulses*

Device	Peak input force (N)	Input acceleration (ms^{-2})	Input velocity (ms^{-1})	Beam acceleration (ms^{-2})	Beam velocity (ms^{-1})
Impulse hammer	240.2 ± 25.5	NA	NA	2,845 ± 346	1.12 ± 0.07
AAI	115.4 ± 8.4	10,725 ± 1,656	1.41 ± 0.32	894 ± 106	18.5 ± 5.79

NA, Not applicable.
Values are expressed as mean ± SD for 10 impulses delivered to 1-m steel beam. Results are shown for AAI device with a 30-durometer rubber tip (30d).

quency. These impedance traces were also ensemble averaged, and the first resonant frequency was obtained graphically as the frequency at which the transfer impedance was minimum (close to zero magnitude). An important parameter associated with the time-domain to frequency-domain conversion described earlier is the frequency resolution (Δf), which is defined as:

$$\Delta f = 1/(\Delta t \cdot N)$$

where Δt is the sampling interval and N is the number of samples. In this study, $\Delta t = 20$ μs and $N = 16{,}384$, resulting in a frequency resolution or frequency interval of approximately 3 Hz.

To quantify the frequency content of the AAI and PCB input forces, two additional parameters were measured from each force magnitude versus frequency plot: (1) the frequency input 3 dB value); and (2) the relative energy of the force input over the range 1 to 150 Hz. The relative input energy was computed as an area ratio FA/OA (expressed as a percentage), where FA is the area under the force magnitude versus frequency curve and OA is the overall area calculated as the peak load magnitude at 3 Hz times 150 Hz. This procedure is graphically illustrated in Fig 5. The rationale for the area ratio measurements will be discussed later.

For each of the additional 5 trials conducted for the 3 subsets of data (eg, effects of tip durometer, stylus mass, and force setting), the relative energy FA/OA produced by the AAI input force magnitude was analyzed. Preliminary results for tests conducted with a "preload-control frame" attached to the AAI are also discussed.

RESULTS

Mean peak force, acceleration, and velocity imparted by the PCB and the AAI are summarized in Table 2. Peak input forces obtained from the PCB were approximately twice as high as those obtained from the AAI. Both devices imparted a consistent peak input force to the beam as indicated by the relatively low coefficients of variation (coefficients of variation = SD/mean) obtained for the 10 impulses: 10.6% and 7.2% for the PCB hammer and AAI, respectively. Note that the PCB produces a very nearly half sine wave impulse with a duration of approximately 0.5 ms, whereas the AAI impact consists of several peaks including a primary peak (peak 1) with a duration of <0.1 ms followed by a secondary main peak (peak 2) with a duration of approximately 5 ms. The PCB tended to impart more acceleration but roughly similar velocity to the beam compared with the AAI. The acceleration measured at the stylus of the AAI was approximately 10 times greater than the acceleration response of the beam.

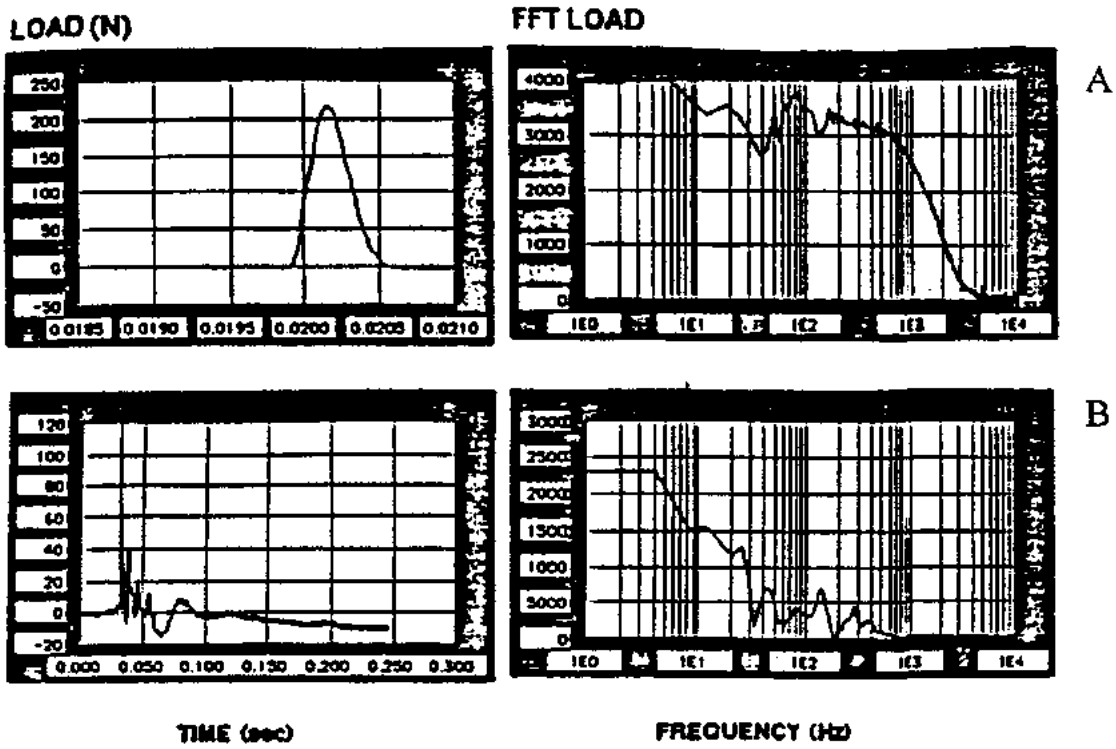

Fig 6. *Typical force-time and force-frequency characteristics obtained for impulse hammer* ***(A)*** *and AAI device* ***(B)****. FFT spectrum frequency axis is log scale.*

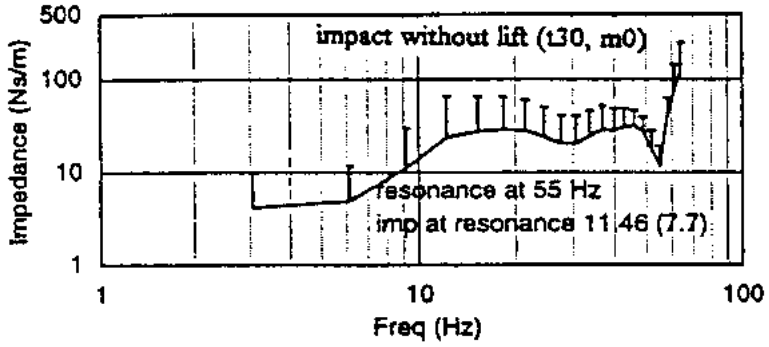

Fig 7. *Ensemble averaged driving point impedance (Z_0) versus frequency curves derived from time-to-frequency domain conversion of AAI force and velocity versus time curves. Both impedance and frequency axes are log scale.*

Fig 6 illustrates typical force-time and force-frequency characteristics obtained for the PCB and AAI devices. Noteworthy is the fact that the PCB produces a relatively constant force magnitude up to approximately 0.1 kHz, whereas the AAI device shows a much more variable force magnitude over the same frequency range. For the PCB the –3 dB point or f_{50} occurred at 197 Hz and 21%.

Ensemble averaged impedance versus frequency curves derived from the time-to-frequency domain conversion of the force and velocity versus time curves are shown for the AAI in Fig 7. The sudden dip in the impedance spectrum correctly identifies the first natural or resonance frequency (f_n = 56 Hz for the 1-m steel beam). Note that a decrease in mechanical impedance is associated with an increase in the amplitude of oscillations of the structure (decreased stiffness) and rapid phase change, both of which are characteristic of structures that are oscillating at or near the resonant frequency. At the resonant frequency, the driving point mechanical impedance determined from the AAI was Z_0 = 11.46 ± 7.7 Ns/m (coefficient of variation = 67%). The impulse hammer transfer impedance method also correctly identified the resonant frequency (55 Hz) but had much less variability (coefficient of variation = 6%) in the transfer impedance calculated at the resonant frequency (Z_1 = 2.83 ± 0.18 Ns/m) compared with the AAI driving point impedance method. Analysis of the transfer impedance by means of the AAI force and beam acceleration data resulted in a lower variance in the measured impedance at the natural frequency

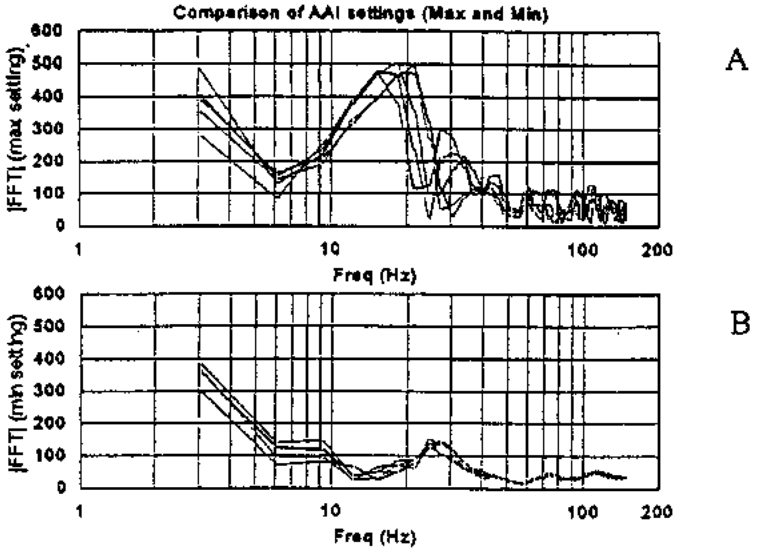

Fig 8. *Frequency characteristics of AAI input force for maximum **(A)** and minimum **(B)** force settings (refer to Fig 2). FFT force magnitude was much greater in the frequency range 10 to 20 Hz. FFT spectrum frequency axis is log scale.*

Table 3. *Comparison of AAI input force frequency characteristics as a function of AAI force setting*

Force setting (reference Fig 2)	Peak 1 force (N)	Peak 2 force (N)	FFT peak magnitude (N)	–3-dB frequency f_{50} (Hz)	Area ratio FA/OA (%)
Minimum	139.3 ± 10.5	33.7 ± 8.1	138.8 ± 9.3	34.8 ± 1.6	15 ± 1
Maximum	115.6 ± 3.5	98.1 ± 8.4	483.4 ± 13.4	24.4 ± 3.1	29 ± 7

Values are expressed as mean ± SD for 5 AAI impulses delivered to 1-m steel beam. All tests were performed with an 80d tip.

Table 4. *Comparison of AAI input force frequency characteristics as a function of tip durometer and added mass*

Tip durometer added mass	30d	50d	70d	80d
m0 (0 g)	26 ± 2	24 ± 5	25 ± 7	25 ± 7
m1 (249 g)	NA	NA	NA	27 ± 6
m2 (386 g)	NA	NA	NA	27 ± 5

NA, Not applicable.

Values are expressed as mean ± SD of area ratio (FA/OA, %) for 5 AAI impulses delivered to 1-m steel beam. All tests were performed at maximum force setting and with 34-g impedance head attached. m0 corresponds to the case with no added mass.

(coefficient of variation = 48%) but underestimated the resonant frequency (f_n = 49 Hz) compared with the driving point method.

Table 3 presents the peak 1 and peak 2 force amplitudes (time domain values) associated with the 2 AAI force settings examined. Note that although the peak 1 force amplitude was fairly similar for both settings, the peak 2 force amplitude at the maximum setting (109 N) was nearly 3-fold greater than the peak 2 force amplitude at the minimum setting (39 N). There was also a marked change in the force frequency spectrum for the 2 AAI force settings over the force frequency range 3 to 150 Hz (Fig 8). Here the force magnitude refers to FFT magnitude of the force spectrum obtained by a root-mean-square summation of all force components with a common frequency (in this case approximately 20 Hz). The peak magnitude of the force is therefore representative of the total energy produced by the AAI for a given frequency. When the force setting was a minimum (setting No. 1 in Fig 2), the mean peak magnitude of the force-frequency spectrum was 139 N (range, 124 to 148 N) and the mean area ratio FA/OA was 15% (range, 14% to 17%) (Table 2). At the maximum force setting (setting No. 3 in Fig 2), the mean peak magnitude of the force-frequency spectrum was 483 N (range, 470 to 503) and the area ratio FA/OA was 29% (range, 23% to 41%).

The force frequency spectrum did not change appreciably with the different durometer tips or masses as shown in Table 4. For all durometer tips and added masses examined, there was a peak at approximately 20 Hz, the signal magnitude decreased to 50% (–3 dB) by 27 to 30 Hz, and the area ratio FA/OA ranged from a minimum of 14% to a maximum of 36%.

DISCUSSION

In this study the force-time and force-frequency characteristics of the AAI were quantified, and the ability of the AAI device to measure the dynamic mechanical properties of an idealized test structure was determined.

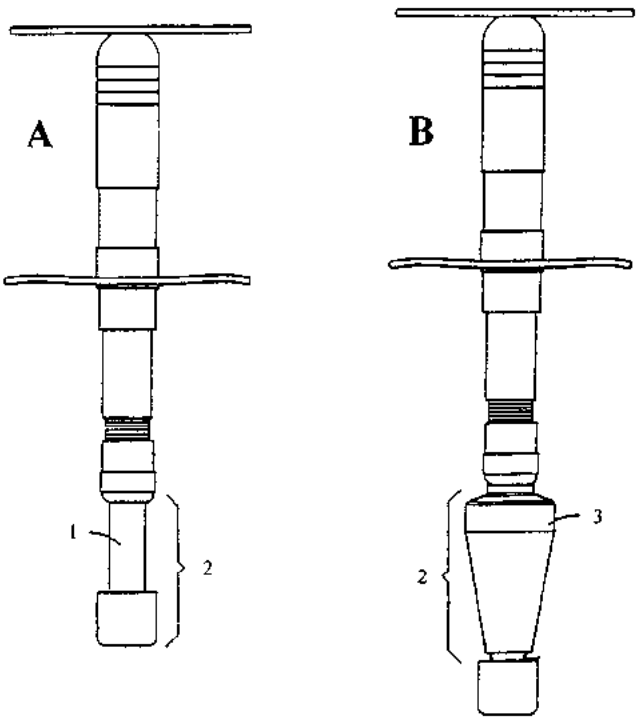

Fig 9. ***A,*** *AAI.* 1, *Shank portion of thrust element;* 2, *thrust element.* ***B,*** *AAI II. Modification of instrument was made by addition of a 45-g stainless steel weight* (3) *to thrust element* (2)*.*

Input Force Amplitude and Frequency Characteristics

The AAI thrust has been described as a high-velocity, relatively low-force impact and is routinely used in SMT.[15] Reports in the biomedical and chiropractic literature have discussed the clinical use of the AAI and Activator Methods Chiropractic Technique.[16-31] Survey reports have indicated that the AAI is estimated to be in use by more than half of all chiropractic practitioners.[32] Therefore the mechanical characteristics of the device are of interest to researchers and clinicians.

Unfortunately, previous descriptions of the AAI force-time characteristics have not been accurately reported. Most notably, Kawchuk and Herzog[33] reported that the peak force and duration of the AAI were 41 N and 32 ms, respectively. This force amplitude is significantly lower than the values reported in this and other studies of the AAI[7] and is more consistent with the peak 2 values reported in this study (34 to 98 N). Presumably, therefore, these authors did not sample the AAI signal with a sufficiently small sampling interval.

In this study we provide a detailed analysis of the force and frequency characteristics of the AAI using a sampling interval of 20 μs/sample. The significant findings include the observation that there is a much higher force component of the AAI, which is easily overlooked by undersampling the force signal. This higher force component is of a very brief duration (<0.1 ms) and therefore produces a very high force impulse (on the order of 1000 kN/s), which is several orders of magnitude greater than other SMT procedures. The secondary AAI peaks have a lower force but are of longer duration (on the order of milliseconds) and therefore contribute more energy to the impact. This is evident when one compares the dynamic mechanical characteristics of the AAI's low (setting No. 1 in Fig 2) and high force settings (setting No. 2 in Fig 2). Both settings produce similar peak forces, but the higher force setting produced 3 times greater peak force magnitude (FFT or frequency domain peak magnitude) than the lower force setting. The higher force setting also contained considerably more energy between 10 and 20 Hz than the lower force setting as is evident from the area ratio FA/OA calculations.

Mechanical Impedance

In this article, we presented 2 methods to assess the dynamic mechanical characteristics of structures, driving-point impedance, and transfer impedance. Driving-point impedance is a method to quantify the force/velocity or mechanical impedance characteristics of a structure at the point of application of the force and is therefore fundamentally different from transfer or transmissibility methods that measure the response characteristics (ie, velocity) at a point different from the point of force excitation (refer to Fig 4). In general, transfer impedance is considered the ideal method to measure the mechanical response of any system because it measures the oscillatory response independently of the input force. However, the transmissibility technique requires attachment of a motion sensor (accelerometer or other transducer) directly to the structure of interest, and therefore transmissibility or transfer measurements necessitate a surgical procedure and are not practical for routine clinical assessment of spinal biomechanics.[7] Mechanical assessment methods that examine the input force and oscillatory response at the point of application of the force (eg, driving point impedance) therefore offer significant advantages in terms of ease of use, particularly in clinical applications such as SMT.

Ideally, an impactor used for dynamic structural testing should excite the structure with a uniform force amplitude over the frequency range of interest. The general rule of thumb is to choose an impactor that delivers an input force-frequency spectrum that is decreased by no more than –20 dB or 10-fold at the maximum frequency of interest. Above this frequency the impactor is less effective in exciting vibrations in the structure. The effective frequency range can be increased by decreasing the time duration of the force impulse, which is accomplished by using a stiffer tip or a lower mass.[34] The impactor should also deliver enough force to produce a measurable response. In this study we examined the effects of tip durometer (a measure of rubber stiffness), added mass, and force magnitude on the input force-frequency characteristics and mechanical impedance associated with an AAI. Although tip durometer and added mass did not show any appreciable effect on the frequency characteristics of the AAI force spectrum, the AAI force ring setting had a marked influence on both the peak 2 force amplitude and the magnitude of FFT force spectrum. Both the low-force and high-force settings of the AAI, however, produced frequency spectrums that decayed rapidly in magnitude greater than 20

to 30 Hz. Indeed, the force magnitude was decreased by more than –20 dB by 55 Hz, which was the theoretical and experimentally determined resonant frequency of the steel test beam. It is not surprising, therefore, that mechanical impedance values derived from analysis of the AAI force/velocity spectrum showed considerable variability.

Another important consideration regarding assessment of mechanical properties of biologic or man-made structures is to ensure that each impact is essentially the same in terms of the position and orientation of the impact relative to the surface (not so much in magnitude because this is accommodated in the force-response process). This may be another source of some of the variability observed in the driving point mechanical impedance measurements derived from the AAI (>70% variability in mechanical impedance at resonance), which relies on the operator's ability to reproduce position, preload, and control the impact during use. All the tests were performed by the same operator and used a low preload. Although care was taken to position the AAI at the same location and along the same direction (perpendicular to the beam length and width), recoil from the AAI hammer and rebound from the steel beam after the impulse may have contributed to some of the variability observed in the magnitude of the impedance. A target was located on the beam to indicate the desired point of contact, but no vertical positioning feedback devices were used for either the AAI or PCB measurements.

Another attribute of the PCB is the fact that it does not remain in contact with the test structure and also uses an electromechanical mechanism to move the stylus into contact with the test structure, both of which may have contributed to the excellent test reproducibility observed (<10% variability in mechanical impedance at resonance). The PCB provided a more reproducible measure of transfer impedance as indicated by the low coefficients of variation obtained for the peak force and impedance magnitude measurements and should be regarded as the "gold standard." Noteworthy, however, was the finding that both the PCB and the AAI methods precisely predicted the theoretical first natural or resonant frequency of the test structure.

In this study we have performed our experiments and analyses with a steel beam test specimen rather than a human or animal test subject. Consequently, the results presented in this article do not directly pertain to SMT and studies of the loading characteristics associated with SMT. Although this may be considered a limitation in terms of clinical applicability, the choice of a steel beam rather than a biologic structure as a test bed for the mechanical impedance measurements offers several advantages. First, the steel beam has a simplified geometry and composition compared with biologic structures, which makes experimental and theoretical determination of the static and dynamic mechanical properties straightforward. In this case we were able to precisely determine that the beam had a static structural stiffness, elastic modulus, and dynamic resonant frequency of 46 kN/mm, 167 GPa, and 56 Hz, respectively. Noteworthy is the fact that the flexural stiffness of the steel beam was chosen to mimic the normal PA stiffness of the human spine. This experimental and theoretical information could then be compared with values derived with the PCB and AAI. Second, the effects of storage and handling on the mechanical response of the beam were not of concern as would be the case for biologic tissues. Finally, viscoelastic effects or time-dependent changes in mechanical properties associated with temperature, loading rate, and type of loading were not factors as would be the case in biologic tissues, including the spine.[35-37] However, it is important to point out that the dynamic mechanical impedance method described is general enough to the extent that the ability to characterize the dynamic structural mechanical behavior of an engineering material like steel can be readily extended to characterization of the dynamic structural mechanical behavior of biologic structures, including the spine.

Assessment of Spinal Stiffness

On the basis of clinical results obtained with the driving point impedance approach, Nathan and Keller[7] and Keller[13] proposed that approximately instrumented mechanical devices such as the AAI, in combination with a computer-based frequency analysis, may be an effective means to evaluate the biomechanical characteristics of the spine. The results of this study provide additional support for chiropractic-based assessment strategies that use a noninvasive driving point impedance measurement system to probe and quantify the mechanical characteristics of the spine. Thus far, this study has focused on a description of the dynamic mechanical response of a beam structure from the point of view of a parameter called mechanical impedance.

Mechanical impedance has units of Ns/m, which is the force measured in newtons divided by the velocity measured in meters per second. For a given frequency in the impedance spectrum, one can derive an "effective" mechanical stiffness by simply multiplying the impedance by the circular frequency $\omega = 2\pi f$, where f is the frequency in Hz and ω has units of radians per second. The resulting effective mechanical stiffness has units of N/m and can be computed for any frequency of interest. Mechanical stiffness values calculated in this manner for frequencies ≤1.0 Hz would provide information regarding the quasistatic mechanical behavior of the structure, whereas values for higher frequencies provide information concerning the dynamic mechanical behavior of structures. In this study the DC term or static effective mechanical stiffness derived from the AAI driving point impedance measurements was 22 kN/m (refer to Fig 7, *A*). The latter corresponds reasonably well with the static flexural stiffness of the steel beam derived experimentally (46 kN/m). Differences between the driving point frequency spectrum analysis results and experimental beam flexural test results are most likely caused by the presence of the AAI rubber tip, which is deformed during the application of the force impulse. Stiffer tips (eg, 80d or greater) are therefore recommended for quantifying structural stiffness with the driving point impedance technique.

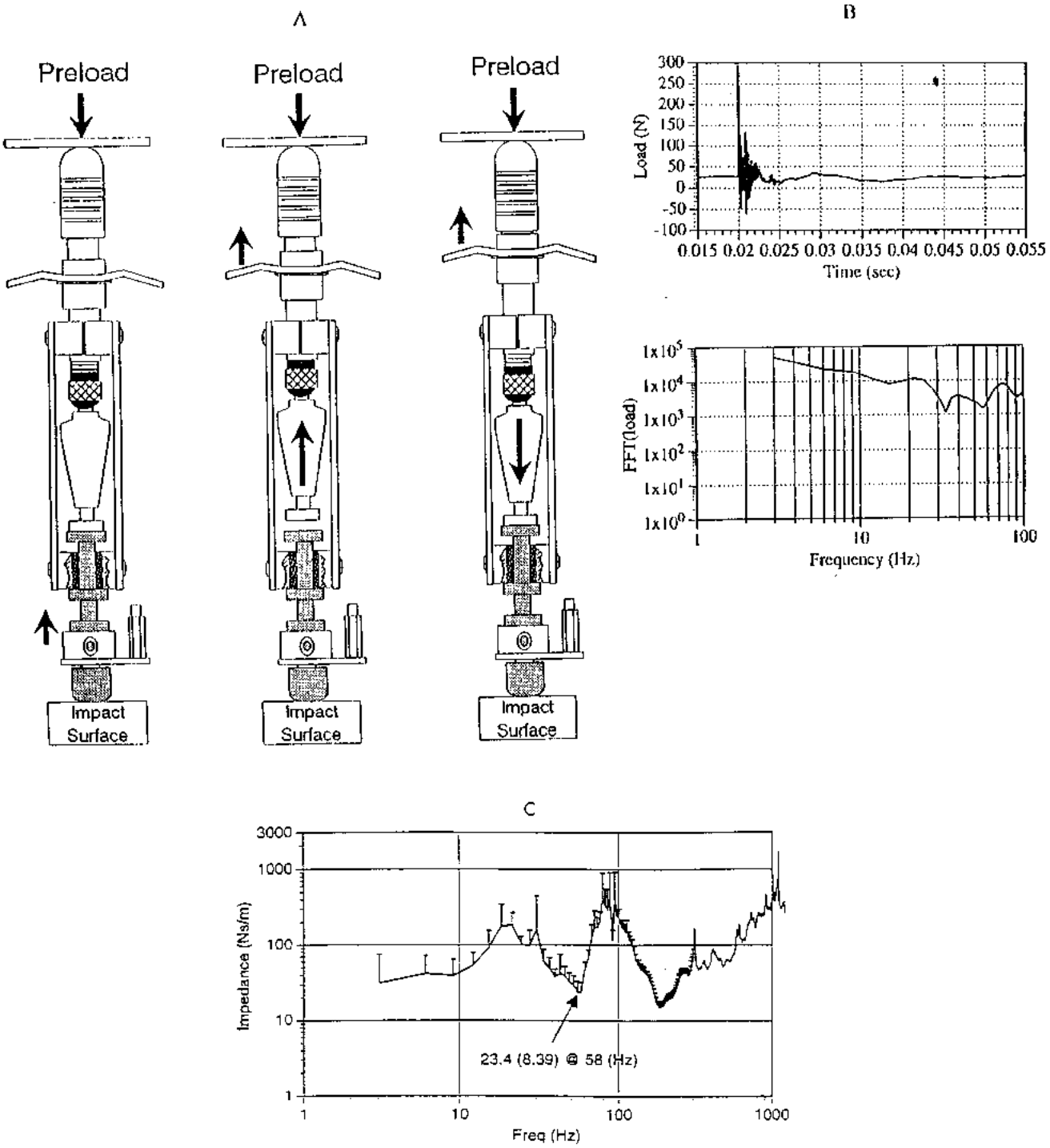

Fig 10. ***A,*** *Schema of a prototype AAI device with support frame for mechanical impedance analysis.* ***B,*** *Force-time and force-frequency spectrum characteristics (log-log scale) of prototype AAI device shown in* ***A****. Test conducted on 1-m steel beam.* ***C,*** *Ensemble averaged driving point impedance (Z_0) versus frequency curves obtained for AAI device with attached isolation frame. Both impedance and frequency axes are log scale.*

Frequency response parameters (impedance, stiffness), together with identification of the resonant frequency associated with oscillations induced by the AAI, can provide clinicians with important information concerning the mechanical behavior of the structure. When the spine is dynamically loaded along the PA direction, a lower impedance and/or stiffness implies that the intervertebral joints are easier to excite and are therefore capable of greater movement or mobility. At the resonant or natural frequency, the spine will be least stiff and will therefore have the greatest potential for mobility, as much as 3 times greater than the mobility at other frequencies.[13] From a therapeutic point of

view, one clinical implication of enhanced mobility is the fact that the mechanical response (motion) of the spine will be maximized for a given force when that force is delivered at the resonant frequency. For example, a force of 150 N delivered at the resonant frequency will produce the same FSU movements as a 450-N force delivered at some other frequency. SMT procedures that impart forces containing a wide spectrum of frequencies may maximize the oscillatory response of the spine. Physiologic responses of the spinal ligaments, intervertebral disks, facet capsules, paraspinal musculature, and other surrounding tissues may also be influenced by the frequency content of the force impulse delivered to the spine during SMT. From a diagnostic point of view, knowledge of the dynamic characteristics of the spine may be useful for identifying the location and quantifying the severity of spinal joint dysfunction or spinal abnormalities.

Improvements in the Force-Frequency Spectrum of the AAI

Although the results obtained were encouraging, from the point of view of determination of the dynamic mechanical characteristics of the AAI compared with the electronic impulse hammer, we were prompted to investigate alternatives to enhance the force-frequency spectrum of the AAI. Current clinical versions of the Activator II Adjusting Instrument (AAI II) incorporate an additional integral mass (about 45 g) attached to the stylus, which alters the force-time profile and consequently the input force-frequency characteristics of the device toward a more uniform frequency spectrum compared with the original AAI device (Fig 9). Other modifications to the AAI II that have been sought to make the AAI impedance measurements more reproducible include incorporation of a preload control frame that isolates the load cell and accelerometer from the AAI stylus and eliminates any influence that preload and hammer recoil may have on the force profile and subsequent force and acceleration measurements (Fig 10, *A*).

Preliminary tests performed on the steel beam indicate that the addition of the preload control frame preserves a greater than –20-dB signal amplitude degradation over the frequency range 10 to 100 Hz (Fig 10, *B*). Results of 10 trials on the 1-m steel beam resulted in a mean impedance of 23.4 Ns/m and a coefficient of variation of 36% (SD, 8.4) at the measured resonant frequency (58 Hz) (Fig 10, *C*). These results demonstrate the enhancement of the force-frequency spectrum of the instrument with this modification. At present, we are performing clinical trials with this device on a cohort of symptomatic and asymptomatic human volunteers.

CONCLUSION

This study indicates that the AAI combined with an integral load cell and accelerometer was able to obtain an accurate description of a steel beam with readily identifiable dynamic mechanical properties. The addition of a preload-control frame to the AAI improved the characteristics of the force-frequency spectrum and repeatability of the driving point impedance measurements. These findings support the rationale for using the device to assess the dynamic mechanical behavior of the vertebral column.

For successful and routine clinical use of spine biomechanical analyses, a given method should be noninvasive, reproducible, inexpensive, simple to operate, and painless in application. The impedance measurement and analysis procedure described here appear to satisfy these requirements. By modifying the force and frequency characteristics of the AAI and other SMT instruments, impedance measurements may not only be used to evaluate the dynamic stiffness characteristics of the spine but may also be more effective while simultaneously providing treatment. Noteworthy in this regard is that the frequency content of the force input is hypothesized to play an important role in a variety of physiologic processes, including healing and regulation of tissue mass, excitation of mechanosensitive afferents, reflexogenic responses, and anti-inflammatory mechanisms, which are currently hypothesized to play an important role in pain modulation and systemic health.[38-45] Consequently, precisely tuned mechanical impulse delivery devices not only may be used to evaluate the dynamic mechanical stiffness characteristics of the human spine but may also be able to maximize therapeutic effects and benefits while reducing the risk of iatrogenic injury. The dynamic measurement techniques presented in this study are currently being used to study the in vivo mechanical characteristics of the normal and pathologic human spine.

ACKNOWLEDGMENTS

We thank James Lehneman for his numerous contributions to this work.

REFERENCES

1. Hessel BW, Herzog W, Conway PIW, McEwen MC. Experimental measurement of the force exerted during spinal manipulation using the Thompson technique. J Manipulative Physiol Ther 1990;13:448-53.
2. Kawchuk GN, Herzog W, Hasler EM. Forces generated during spinal manipulative therapy of the cervical spine. J Manipulative Physiol Ther 1992;15:275-8.
3. Lee RYW, Evans JH. Load-displacement-time characteristics of the spine under posteroanterior mobilization. Aust J Physiother 1992;38:115-23.
4. Herzog W, Conway PJ, Kawchuk GN, Zhang Y, Hasler EM. Forces exerted during spinal manipulative therapy. Spine 1993;18:1206-12.
5. Gál J, Herzog W, Kawchuk GN, Conway PJ, Zhang YT. Biomechanical studies of spinal manipulative therapy (SMT): quantifying the movements of vertebral bodies during SMT. J Can Chiropract Assoc 1994;38:11-24.
6. Lee M, Lau H, Lau T. Sagittal plane rotation of the pelvis during lumbar posteroanterior loading. J Manipulative Physiol Ther 1994;17:149-55.
7. Nathan M, Keller TS. Measurement and analysis of the in vivo posteroanterior impulse response of the human thoraco-lumbar spine: a feasibility study. J Manipulative Physiol Ther 1994; 17:431-41.
8. Wood J, Adams AA, Hansmeier D. Force and time characteristics of Pierce technique cervical adjustments. J Chiropract Res Clin Invest 1994;9:39-44.
9. Gál J, Herzog W, Kawchuk G, Conway PJ, Zhang YT. Move-

ments of vertebrae during manipulative adjustments to unembalmed cadavers. J Manipulative Physiol Ther 1997;20:30-40.
10. Lee M, Latimer J, Maher C. Normal response to large posteroanterior lumbar loads: a case study approach. J Manipulative Physiol Ther 1997;20:369-71.
11. Triano J, Schultz AB. Loads transmitted during lumbosacral spinal manipulation therapy. Spine 1997;22:1955-64.
12. Pipher WL. Clinical instability of the lumbar spine. J Manipulative Physiol Ther 1990;13:482-5.
13. Keller TS. In vivo transient vibration analysis of the normal human spine. In: Fuhr AW, Colloca CJ, Green JR, Keller TS, editors. Activator methods chiropractic technique. St. Louis: Mosby–Year Book; 1997. p. 431-50.
14. Osterbauer PJ, Fuhr AW, Keller TS. Description and analysis of Activator methods in chiropractic technique. In: Lawrence DJ, Cassidy JD, McGregor M, Meeker WC, Vernon HT, editors. Advances in chiropractic. St. Louis: Mosby–Year Book; 1996. p. 471-520.
15. Osterbauer PJ, Fuhr AW, Hildebrandt RW. Mechanical force, manually assisted, short lever chiropractic adjustment. J Manipulative Physiol Ther 1992;15:309-17.
16. Fuhr AW, Colloca CJ, Green JR, Keller TS, editors. Activator methods chiropractic technique. St. Louis: Mosby–Year Book; 1997.
17. Osterbauer PJ, Fuhr AW. The current status of Activator methods chiropractic technique, theory, and training. Chiropract Technique 1990;21:168-75.
18. Cooperstein R. Activator methods chiropractic technique. Chiropract Technique 1997;9:108-14.
19. Frach JP, Osterbauer PJ, Fuhr AW. Treatment of Bell's palsy by mechanical force, manually assisted chiropractic adjusting and high-voltage electrotherapy. J Manipulative Physiol Ther 1992;15:596-8.
20. Yates RG, Lamping DL, Abram NL, Wright C. Effects of chiropractic treatment on blood pressure and anxiety: a randomized controlled trial. J Manipulative Physiol Ther 1988;11:484-8.
21. Yurkiw D, Mior S. Comparison of two chiropractic techniques on pain and lateral flexion in neck pain patients: a pilot study. Chiropract Technique 1996;8:155-62.
22. Osterbauer PJ, Derickson KL, Peles JD, DeBoer KF, Fuhr AW, Winters JM. Three-dimensional head kinematics and clinical outcome of patients with neck injury treated with spinal manipulative therapy: a pilot study. J Manipulative Physiol Ther 1992;15:501-11.
23. Polkinghorn BS. Treatment of cervical disc protrusions via instrumental chiropractic adjustment. J Manipulative Physiol Ther 1998;21:114-21.
24. Polkinghorn BS. Posterior calcaneal subluxation: an important consideration in chiropractic treatment of plantar fasciitis (heel spur syndrome). Chiropract Sports Med 1995;9:44-51.
25. Polkinghorn BS. Conservative treatment of torn medial meniscus via mechanical force, manually assisted short lever chiropractic adjusting procedures. J Manipulative Physiol Ther 1994;17:474-84.
26. Richards GL, Thompson JS, Osterbauer PJ, Fuhr AW. Low force chiropractic care of two patients with sciatic neuropathy and lumbar disc herniation. Am J Chiropract Med 1990; 3(1):25-32.
27. Gemmell HA, Jacobson BH. The immediate effect of activator vs. meric adjustment on acute low back pain: a randomized controlled trial. J Manipulative Physiol Ther 1995;18:453-6.
28. Osterbauer PJ, DeBoer KF, Widmaier RS, Petermann EA, Fuhr AW. Treatment and biomechanical assessment of patients with chronic sacroiliac joint syndrome. J Manipulative Physiol Ther 1993;16:82-90.
29. Polkinghorn BS, Colloca CJ. Treatment of symptomatic lumbar disc herniation utilizing activator methods chiropractic technique. J Manipulative Physiol Ther 1998;21:187-96.
30. Polkinghorn BS. Chiropractic treatment of frozen shoulder syndrome (adhesive capsulitis) using mechanical force manually assisted short lever adjusting procedures. J Manipulative Physiol Ther 1995;18:105-15.
31. Polkinghorn BS. Instrumental chiropractic treatment of frozen shoulder associated with mixed metastatic carcinoma. Chiropract Technique 1995;7:98-102.
32. Christensen MG, Delle Morgan DR. Job analysis of chiropractic: a project report, survey analysis and summary of the practice of chiropractic within the United States. Greeley (CO): National Board of Chiropractic Examiners; 1993.
33. Kawchuk GN, Herzog W. Biomechanical characterization (fingerprinting) of five novel methods of cervical spine manipulation. J Manipulative Physiol Ther 1993;16:573-7.
34. Ewins DJ. Modal testing: theory and practice. Hertfordshire, England: Bruel and Kjaer; 1986.
35. Keller TS, Spengler DM, Hansson TH. Mechanical behavior of the human lumbar spine. I. Creep analysis during static compressive loading. J Orthop Res 1987;5:467-78.
36. Hansson TH, Keller TS, Spengler DM. Mechanical behavior of the human lumbar spine. II. Fatigue strength during dynamic compressive loading. J Orthop Res 1987;5:479-87.
37. Keller TS, Holm SH, Hansson TH, Spengler DM. The dependence of intervertebral disc mechanical properties on physiological conditions. Spine 1990;15:751-61.
38. Gillette RG. A speculative argument for the coactivation of diverse somatic receptor populations by forceful chiropractic adjustments. Manual Med 1987;3:1-14.
39. Pickar JG, McLain RF. Responses of mechanosensitive afferents to manipulation of the lumbar facet in the cat. Spine 1995;20:2379-85.
40. Korr IM, ed. Neurobiologic mechanisms in manipulative therapy. New York: Plenum Publishing; 1978.
41. Wyke BD. Articular neurology and manipulative therapy. In: Glasgow EF, et al, editors. Aspects of manipulative therapy. 2nd ed. New York: Churchill Livingstone; 1985.
42. Sato A. Somatovisceral reflexes. J Manipulative Physiol Ther 1995;18:597-602.
43. Sato A. The reflex effects of spinal somatic nerve stimulation on visceral function. J Manipulative Physiol Ther 1992;15:57-61.
44. Cavanaugh JM, Ozaktay AC, Yamashita HT, King AI. Lumbar facet pain: biomechanics, neuroanatomy and neurophysiology. J Biomechanics 1996;29:1117-29.
45. Cavanaugh JM. Neural mechanisms of lumbar pain. Spine 1995;20:1804-9.